Chemical Engineering Journal 371 (2019) 130–137

Contents lists available at ScienceDirect

Chemical Engineering Journal

journal homepage: www.elsevier.com/locate/cej

Facile preparation of photonic and magnetic dual responsive protein imprinted nanomaterial for specific recognition of bovine hemoglobin

Xiaoyu Xie[a,b], Qi Hu[a,b], Ruifang Ke[a,b], Xueyan Zhen[a,b], Yusi Bu[a,b], Sicen Wang[a,b,*]

[a] School of Pharmacy, Health Science Center, Xi'an Jiaotong University, Xi'an 710061, China
[b] Shaanxi Engineering Research Center of Cardiovascular Drugs Screening & Analysis, Xi'an 710061, China

HIGHLIGHTS

- Novel photonic and magnetic dual responsive protein MIPs were first prepared.
- A water-soluble azobenzene containing photoswitchable functional monomer was synthesized.
- Outstanding magnetic properties and well selective photoreponsive ability were obtained.
- The MIPs exhibited specific recognition of target protein from real biological sample.

GRAPHICAL ABSTRACT

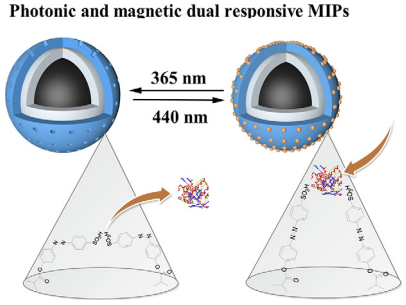

ARTICLE INFO

Keywords:
Dual responsive protein imprinted polymers
Photonic responsive
Magnetic responsive
Bovine hemoglobin

ABSTRACT

Stimulated response molecularly imprinted polymers (MIPs) have attracted wide attention not only because of their intriguing response to external stimuli, but also due to the desired molecular recognition ability. Herein, a novel dual responsive proteins MIPs with both photonic and magnetic stimuli has been developed by surface imprinting polymerization, where double bonds modified Fe_3O_4 nanoparticles, a water-soluble azobenzene containing 4-[(4-methacryloyloxy)phenylazo]benzenesulfonic acid and bovine hemoglobin (BHb) were used as magnetic core, photoswitchable functional monomer and template protein, respectively. The resultant MIPs possessed a typical spherical structure with a relative rough imprinted layer of 15 nm thickness. Moreover, the MIPs had good binding behavior toward BHb with fast binding kinetics, high adsorption capacity and satisfactory selectivity. The MIPs were proved to be well photo-controlled toward the template protein BHb under the alternating irradiation of 365 and 440 nm: 31.4% BHb was released from the MIPs at 365 nm and 67.2% BHb was bound into the MIPs at 440 nm. As a result, the MIPs were successfully applied to specifically extract template protein from actual biological sample. As a consequence, combining photocontrolled release and uptake, rapidly magnetic separation and specific recognition, the resultant MIPs with photonic and magnetic dual responsive abilities show significant advantages in the enrichment of trace protein in biological samples.

1. Introduction

As an iron-containing oxygen-transport metalloprotein, hemoglobin (Hb) plays a vital role in numerous physiological activities, and liable for transport of oxygen, carbon dioxide and nitric oxide [1,2]. Too high or low Hb levels would lead to various diseases, such as anemia [3], diabetes [4], hematemesis [5], hematuria [6], etc. Therefore, the accurate determination of Hb is of essential significance for proteomics

* Corresponding author at: School of Pharmacy, Health Science Center, Xi'an Jiaotong University, Xi'an 710061, China.
E-mail address: wangsc@mail.xjtu.edu.cn (S. Wang).

https://doi.org/10.1016/j.cej.2019.04.019
Received 31 January 2019; Received in revised form 22 March 2019; Accepted 3 April 2019
Available online 04 April 2019
1385-8947/

research in biological systems. For example, Hb in the urine has been demonstrated to be linked to kidney stones, renal cancer and other diseases [7], and Hb in gastric intestine fluids has clinicopathologic significance for hemorrhages from ulcers, tumors and additional ailments [8]. Bovine hemoglobin (BHb) has been used as the alternative protein of Hb because of the high similarity (90%) between BHb and Hb [2,9]. Currently, the accuracy and sensitivity of protein detection are generally limited by the complex matrices and low abundance of protein biomarkers [10,11]. To enhance the present detection toward target proteins, it is urgent to develop an effective technique with high selectivity for target proteins and excellent tolerance for interference of complex matrices.

In the past decades, molecular imprinting has increasingly been an excellent technology for building “plastic antibodies” with a great potential in varieties of fields, especially in the health and life sciences [12,13]. With this tool, new artificial mimicking binding sites have been constructed with appreciable selectivity, excellent stability and inexpensive preparation costs, which are chemically and sterically complementary to template molecule [14,15]. So far, small molecules imprinting has been hugely successful and some even to an industrial level [16,17], whereas the creation of molecularly imprinted polymers (MIPs) for biomacromolecules such as protein still faces with great challenges under the influences of macromolecular size, structure complexity, conformation flexibility and solubility [18,19]. To solve these problems, some protein imprinting techniques have been achieved, including surface imprinting [20], metal-chelating imprinting [21] and epitope imprinting [22], etc. Among these techniques, surface imprinting has been considered a promising strategy because of the imprinted cavities on or close to the surface of MIPs. Moreover, when combined with supporting magnetic nanoparticles, the resultant MIPs not only improve the site accessibility of imprinted cavities, but also have excellent magnetic responsiveness for separation from complex matrix.

Meanwhile, as a class of smart materials, photo-responsive polymers can accomplish photodriven isomerization by transforming the irradiation of light [23,24]. The introduction of photoresponse into magnetic molecularly imprinted polymers brings dual stimuli responsive polymers. On the one hand, the photonic property makes a significant alteration in the imprinted cavities geometry under the ultraviolet radiation, thus causing the template molecule uptake and release [25,26]. On the other hand, the magnetic properties allow rapid separation from complex matrix with an external magnet [27,28]. In the process of preparation, the photo-responsive functional monomers, always containing azobenzene chromophore, have been applied [25]. As is well known, most of the reported imprinted materials were prepared using traditional functional monomers in organic media [16], which restricted the application of protein molecular imprinting because of solubility of proteins [29]. Among the single signal responsive protein imprinting techniques, magnetic response has received extensive attention [18]. Meanwhile, although dual and multi stimuli responsive protein imprinted polymers have been explored, such as magnetic and pH dual response [29] and magnetic, environmental temperature and pH multi response [30], combing magnetic and photonic response has not been reported in preparation of protein imprinted polymers. To this end, we aim to prepare dual responsive protein MIPs with photonic and magnetic responses, where a water-soluble azobenzene-containing functional monomer was applied. As far as we know, the construction of magnetic and photonic dual responsive MIPs of any proteins has never been reported.

Herein, we developed a facile and reliable approach of surface imprinting to prepare the protein imprinted polymers with photonic and magnetic dual responsive ability for specific recognition of BHb. Functionalized Fe_3O_4 was synthesized as a support for rapidly magnetic separation and a photoswitchable functional monomer with good water solubility, 4-[(4-methacryloyloxy)phenylazo]benzenesulfonic acid (MAPASA), was synthesized for imprinting proteins in biocompatible aqueous media. The characterization, buffer solution type and pH and adsorption properties of the prepared MIPs were methodically studied. Meanwhile, the photoisomerization reversibility was estimated by the photoregulated uptake and release experiments. Moreover, the practicability of the proposed MIPs was also evaluated by detection of BHb in actual bovine blood sample.

2. Experimental

2.1. Materials and regents

BHb (M_w = 64.0 kDa, isoelectric point (pI) = 6.9), bovine serum albumin (BSA; M_w = 66.4 kDa, pI = 4.9), myoglobin (Mb; M_w = 17.5 kDa, pI = 7.1), ovalbumin (OVA; M_w = 44.5 kDa, pI = 4.7) and lysozyme (Lyz; M_w = 13.4 kDa, pI = 11.2) were purchased from Solarbio Science & Technology Co., Ltd (Beijing, China). Ammonium persulfate (APS), sodium hydrogen sulfite ($NaHSO_3$), 3-methacryloxypropyltrimethoxysilane (MPS) and N,N′-methylenebisacrylamide (MBA) were obtained from Aladdin Co., Ltd (Shanghai, China). Tetraethoxysilane (TEOS), isopropanol, ammonium hydroxide (28%, weight percent), anhydrous toluene and N,N-dimethylformamide (DMF) were provided by Sinopharm Chemical Reagent Co., Ltd (Shanghai, China). All aqueous solutions were prepared by MK-459 Millipore water system (Shandong, China).

2.2. Instrumentation

The morphology was performed with JEOL JEM-2100HR transmission electron microscope (TEM; Tokyo, Japan). Fourier transform infrared spectroscopy (FT-IR) results (4000–400 cm^{-1}) were investigated by a Nicolet Nexus-670 FT-IR spectrometer (Madison, USA). X-ray diffraction (XRD) patterns were investigated via a Bruker XRD with Cu Kα radiation (Bremen, Germany). An Mpms Squid vibrating sample magnetometer (VSM; Ohio, USA) was applied to determine the magnetic properties of obtained products. The ultraviolet-visible (UV) absorption data were recorded by using a Fuli UV1600 spectrophotometer (Zhejiang, China). Electrophoretic analysis was performed using a sodium dodecyl sulfate-polyacrylamide gel electrophoresis (SDS-PAGE) from Junyi Electrophoresis Co., Ltd. (Beijing, China). HPLC analysis was performed on a Shimadzu (Kyoto, Japan) with a Venusil XBP C8 (4.6 × 250 mm, 5 μm) column (Agela Technologies, Tianjin, China). The mobile phase consisted of water with 0.1% trifluoroacetic acid (TFA) (A) and acetonitrile with 0.08% TFA (B). A linear gradient increase of mobile phase from 30 to 65% within 22 min was used with a flow rate of 1.0 mL min^{-1}. The inject volume was 10 μL, and all proteins were detected through a UV detector at 280 nm.

2.3. Preparation of MIPs

Firstly, the Fe_3O_4@SiO_2 magnetic nanoparticles were synthesized according to a previously published article in our laboratory [31]. The specific steps were elaborated in Supporting Information. Then MPS was used to modify the obtained magnetic nanoparticles according to the reported method [32] with some modification. Briefly, Fe_3O_4@SiO_2 nanoparticles (500 mg) were ultrasonically scattered in anhydrous toluene (100 mL) for 30 min. After adding 5 mL of MPS dropwise, the mixed solution was refluxed for 24 h at 90 °C. The whole reaction was carried on under nitrogen protection. Finally, the surface modified magnetic nanoparticles (Fe_3O_4@SiO_2-MPS) were magnetically collected, rinsed with ethanol and vacuum-dried at 40 °C.

The photo-responsive monomer MAPASA was synthesized according to a previous method [33]. The specific procedures were described in Supporting Information. The photonic and magnetic dual responsive BHb MIPs were synthesized in the dark condition as follows: after dissolving 30 mg of BHb and 173 mg of MAPASA in 15 mL of Tris HCl buffer (pH = 7.0, 10 mM), the mixed solution was stored at room

temperature for 12 h in the dark. Then, the obtained Fe_3O_4@SiO_2-MPS nanoparticles (200 mg) were dispersed in the above mixed solution by vortex and ultrasonic vibration for 30 min, in which the ultrasonic vibration was conducted in ice bath as a complement to improve dispersion. Subsequently, MBA (200 mg), APS (100 mg) and $NaHSO_3$ (15 mg) were dissolved in the mixed solution, which was then mechanically stirred for 24 h at 40 °C in the dark. The precipitation was collected magnetically and then rinsed successively with 2% SDS-HAc solution and deionized water until no adsorption was detected by UV–vis spectroscopy at 410 nm. As the reference, non-imprinted polymers (NIPs) were synthesized under the identical conditions without template protein.

2.4. Binding experiment

In the adsorption kinetics tests, 10 mg of MIPs or NIPs were scattered in 0.5 mg mL^{-1} of BHb Tris-HCl buffer (pH = 7.0, 10 mM) solution (5 mL). Then different incubated time (5–180 min) was investigated at room temperature in the dark. After magnetically isolated the solid particles, the amount of BHb in solution was analyzed by UV–vis spectroscopy, respectively.

The static adsorption tests were conducted by dispersing 10 mg of MIPs or NIPs in 5 mL of BHb Tris-HCl buffer (pH = 7.0, 10 mM) solution with a series of concentrations (0.01–0.9 mg mL^{-1}). Then the mixed solution was incubated for 3 h at room temperature in the dark. After magnetically isolated the solid particles, the amount of BHb in solution was also measured by UV–vis spectroscopy, respectively.

The selectivity tests were evaluated toward 0.5 mg mL^{-1} of BHb, BSA, Mb, OVA and Lyz in Tris-HCl buffer (pH = 7.0, 10 mM), respectively. The operating conditions were consistent with the static adsorption tests. After magnetically isolated the solid particles, the concentrations of five proteins in solution were measured by UV–vis spectroscopy at 410, 280, 410, 275 and 281 nm for BHb, BSA, Mb, OVA and Lyz, respectively.

The adsorption amount of protein (Q, mg g^{-1}) bound to the obtained materials was calculated by the following equation

$$Q = (C_i - C_e)V/W \quad (1)$$

where C_i (mg mL^{-1}) and C_e (mg mL^{-1}) represent the protein concentrations in the initial and equilibrium stages, respectively. V (mL) and W (g) are the volume of sample solution and the mass of adsorbent, respectively.

Moreover, the selectivity of the obtained MIPs was evaluated by the imprinting factor (*IF*) that was calculated by the following equations

$$IF = Q_{MIPs}/Q_{NIPs} \quad (2)$$

where Q_{MIPs} and Q_{NIPs} are the amount of protein adsorbed by MIPs and NIPs, respectively.

2.5. Photoregulated release and uptake studies

Firstly, the stabilities of the four proteins (BHb, BSA, Mb and OVA) under irradiation light at 365 nm and 440 nm were investigated. After irradiated different time (10–120 min), the amount of protein was analyzed by UV–vis spectroscopy, respectively. Secondly, the studies of photoregulated release and uptake were performed on a self-assembled instrument, including a black box, a 5 W 365 nm light source and a 5 W 440 nm light source. Briefly, 10 mg of MIPs were scattered in 5 mL of Tris-HCl buffer (pH = 7.0, 10 mM) containing 0.2 mg mL^{-1} of BHb, BSA, Mb and OVA, respectively. The suspension solution was firstly stirred for 2 h in the dark and the concentrations of the four proteins in solution were analyzed by UV–vis spectroscopy, respectively. In the test of photoregulated release, the suspension solution was irradiated with 365 nm light for 2 h. After isolating the MIPs by a magnetic field, the clear supernatant was analyzed by UV–vis spectroscopy. For the test of photoregulated uptake, the irradiation of 440 nm was used and the following steps were the same as the release study. Irradiation and incubating were started over after the monitoring of the clear supernatant throughout the whole experiment.

2.6. Actual sample application

50 mg of obtained MIPs was scattered in 10 mL of bovine blood sample diluted 150-fold with Tris-HCl buffer (pH = 7.0, 10 mM). The suspension was incubated at room temperature for 30 min in the dark with the help of 440 nm irradiation. After magnetic collection of MIPs, the protein adsorbed on the MIPs was subsequently eluted with 2% SDS-HAc solution under irradiation with 365 nm light for 1 h. Finally, the initial, adsorbed and eluted solutions were examined by SDS-PAGE and HPLC, respectively, and acrylamide was mixed as gel-former (4% (V/V) in the stacking gel and 12% in the separating gel). For the mixed BHb and BSA (0.25 mg mL^{-1} for each) solution, the same experimental conditions were used.

3. Results and discussion

3.1. Preparation of photonic and magnetic dual responsive MIPs

The scheme for synthesis of BHb MIPs with photonic and magnetic dual responsive ability was depicted in Fig. 1. Firstly, Fe_3O_4 nanoparticles were obtained as magnetic core via coprecipitation method to make the obtained products magnetic responsive. Then the silica film was cloaked on the surface of Fe_3O_4 nanoparticles via Stöber method to provide silanol groups, which were subsequently reacted with MPS to introduce the vinyl groups. Finally, imprinted shell could be easily grafted under the copolymerizaiotn of vinyl groups with functional monomer and cross-linker.

MAPASA, a water-soluble photo-responsive functional monomer, was synthesized and the MS, ^{1}H NMR and ^{13}C NMR spectra were given in Figs. S1–S3 in Supporting Information, which was used to recognize and photocontrol template protein binding and release. The photoisomerization properties of MAPASA and the prepared MIPs were characterized. In the trans to cis photoisomerization experiments, MAPASA or the prepared MIPs were dispersed in Tris-HCl buffer (pH = 7.0, 10 mM), which were then irradiated at 365 nm and 440 nm, respectively. As displayed in Fig. S4, a series of strong peaks at 336 nm and some weak ones at 430 nm were obtained, which represented π–π^* and n–π^* electron transitions of the N = N bond in azobenzene, respectively [26]. It was shown in Fig. S4A and B that the MAPASA showed obvious photoisomerization and the values of isomerization rate were comparable to other azobenzene chromophores according to the literature [33,34]. Although, the isomerization intensity of MIPs (Fig. S4C and D) was decreased due to the steric hindrance created by imprinting polymerization with cross-linker, the obtained MIPs still possess satisfactory isomerization to meet the need of photoregulated uptake and release.

3.2. Characterization of the prepared materials

Firstly, the morphology of the Fe_3O_4@SiO_2 and MIPs were shown in Fig. 2a. The as-prepared Fe_3O_4@SiO_2 were spherical particles with a uniform size of 520 nm. After the imprinting process, a relative rough imprinted surface with 15 nm thickness could be obtained (Fig. 2b), suggesting desirable fast mass transfer for template molecule between the imprinted cavities and the solution. Meanwhile, FT-IR was applied to analyze the structure details of Fe_3O_4, Fe_3O_4@SiO_2 and MIPs. As shown in Fig. 3Aa, the strong bands at 580 cm^{-1} corresponded the Fe–O group, indicated the successful synthesis of Fe_3O_4 nanoparticles. Compared with Fig. 3Aa, three new bands at approximately 798, 958 and 1098 cm^{-1} could be attributed to the stretching vibration of Si—O, Si—O—H and Si—O—Si, respectively, confirming Fe_3O_4 nanoparticles were successfully coated by SiO_2 layer (Fig. 3Ab) [17]. The FT-IR

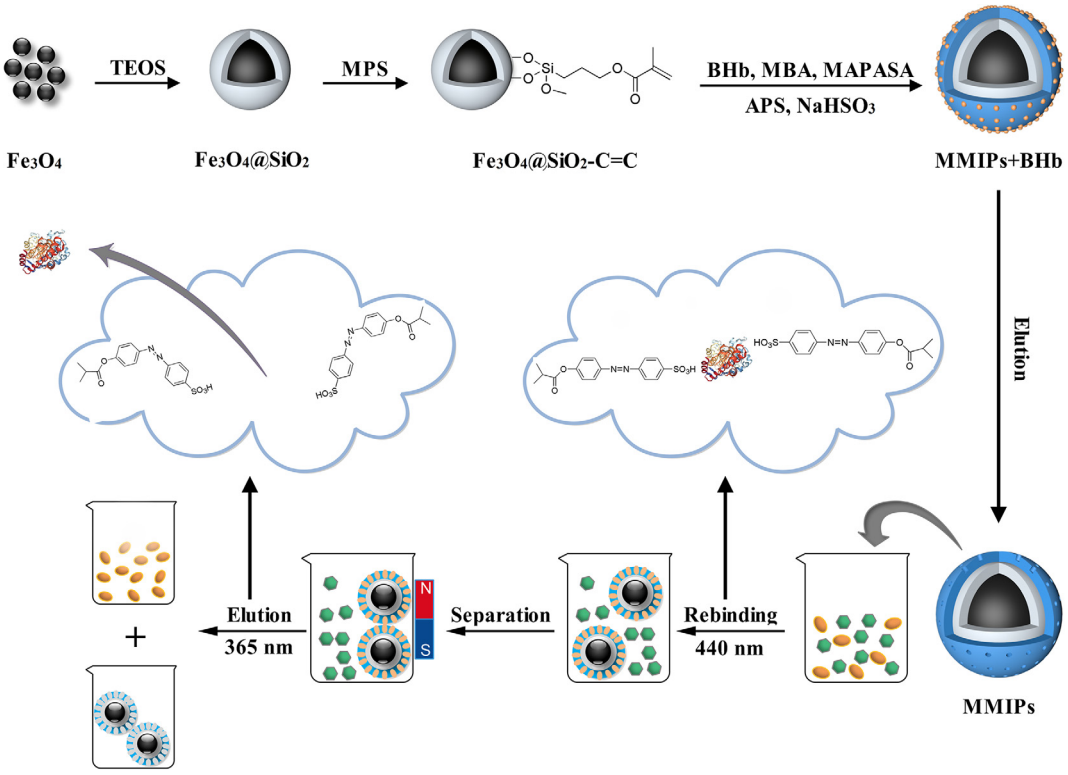

Fig. 1. The schematic illustration of preparation and application of photonic and magnetic dual responsive BHb-MIPs.

spectrum of MIPs (Fig. 3Ac) clearly showed two new characteristic bands at 1730 and 2924 cm^{-1}, originating from the stretching vibration of C═O and C−H, respectively, which could be ascribed to the presence of imprinted layer in the subsequent reactions [32].

The XRD pattern records for Fe_3O_4, Fe_3O_4@SiO_2 and MIPs were displayed in Fig. 3B. For all three samples, the typical peaks of Fe_3O_4 were observed at 2θ values of 30.3°, 35.5°, 43.1°, 53.4°, 57.0° and 62.6° assigned to (2 2 0), (3 1 1), (4 0 0), (4 2 2), (5 1 1) and (4 4 0), respectively, which fit well with the standard XRD data in JCPDS card (19-0629). It can be concluded that the crystal structure of Fe_3O_4 was essentially maintained during the surface functionalization and imprinting process. Moreover, Fig. 3C is the magnetic hysteresis loop of the obtained magnetic nanoparticles. The magnetic saturation values of Fe_3O_4, Fe_3O_4@SiO_2 and MIPs were 65.5, 30.4 and 12.2 emu g^{-1}, respectively. The decrease in magnetic susceptibility may be attributed to the SiO_2 layer and MIPs shell coating, and the magnetic separation experiment results showed that the MIPs could be completely separated from the solution in 15 s with an external magnet. The results revealed that the resulting MIPs have adequate magnetic response to be easily separated with an external magnetic field.

3.3. The optimal buffer solution type and pH

To obtain the best adsorption efficiency, different buffer solution and pH conditions were optimized. First of all, adsorption experiments were employed in Tris-HCl buffer solution (pH = 7.0) and phosphate buffer solution (PBS, pH = 7.0) in the presence of BHb (0.5 mg mL^{-1}), respectively. The MIPs exhibited higher adsorption of BHb in Tris-HCl buffer solution (82.6 mg g^{-1}) than that in PBS (63.1 mg g^{-1}). It should be that PBS has higher ionic strength, hence more buffer ions occupy BHb's cavity through the interaction between charges, which limited the adsorption of BHb by MIPs. Therefore, the optimized buffer solution

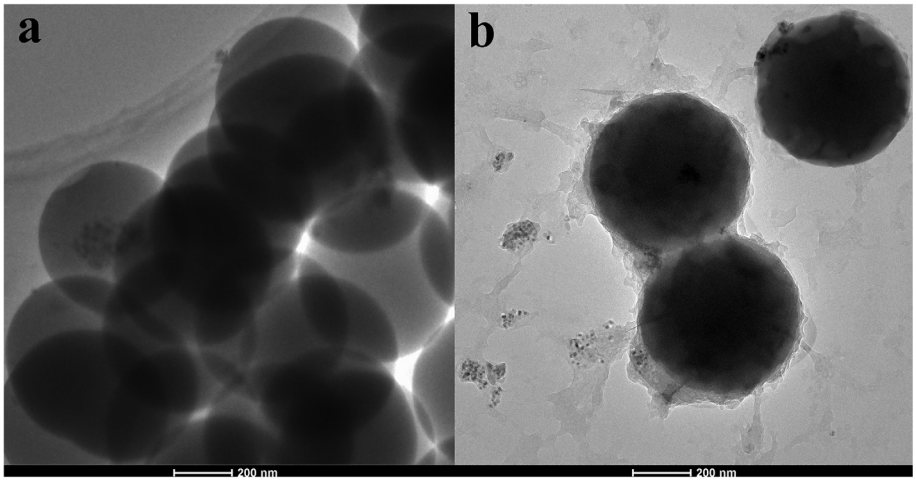

Fig. 2. TEM images of Fe_3O_4@SiO_2 (a) and MIPs (b).

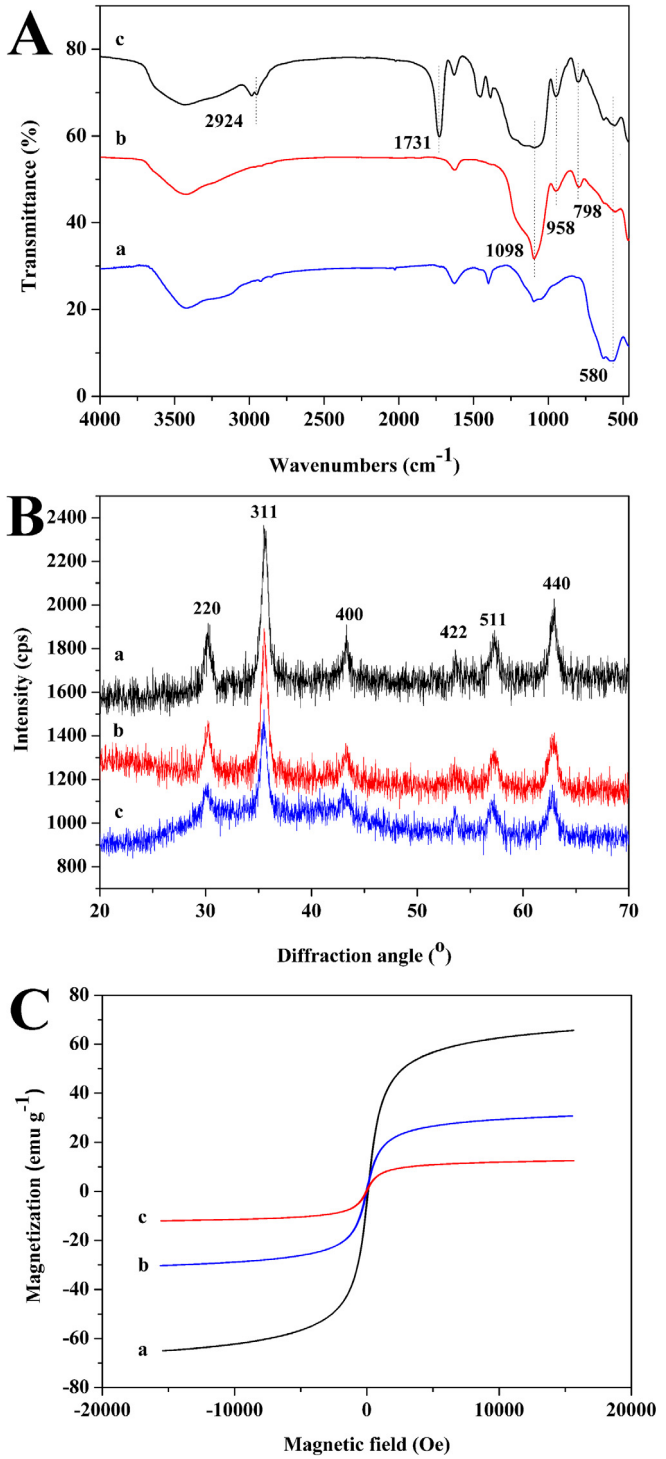

Fig. 3. (A) FT-IR spectra, (B) XRD patterns and (C) Magnetic hysteresis loops of Fe_3O_4 (a), Fe_3O_4@SiO_2 (b), and MIPs (c).

was obtained to be the Tris-HCl buffer solution. Then, a series of adsorption experiments were investigated by varying the pH conditions of Tris-HCl buffer solution from 4.0 to 10.0 containing 0.5 mg mL^{-1} of BHb. Fig. S5 showed that the adsorption capacities of MIPs increased before the pH reached 7.0, then sharply decreased with increasing pH value. On one side, the pI of BHb is about 6.9, when the pH of solution is below 7.0, BHb molecule is positively charged, which could be adsorbed by the negatively charged polymeric MAPASA. When the pH of solution is greater than 7.0, BHb molecule is negatively charged, which blocked the electrostatic interactions between them. On the other side, the structure of the BHb molecule is closely related with its pI. When the pH of solution is at 7.0, the BHb could keep its original structure, which allowed more BHb molecule to enter into the MIP films. For the NIPs, the similar adsorption trend was observed, which was dramatically lower than that of MIPs. It is considered that the BHb molecule was adsorbed onto the NIPs due to the electrostatic interaction between polymeric MAPASA and BHb. Therefore, the value of pH was selected as 7.0 for the subsequent adsorption experiments considering the *IF* and adsorption capacity.

3.4. Binding kinetics

The adsorption efficiency of obtained MIPs was also investigated by the binding kinetics experiments. The kinetic adsorption curves of BHb combined with MIPs or NIPs were exhibited in Fig. 4A. It was clear that BHb bound onto MIPs had a rapid rate within 20 min, then slowing down gradually until the equilibrium was reached. Although a similar adsorption curve of BHb onto NIPs was obtained, the *Q* of which was much lower than that of MIPs. It was indicated that the surface of MIPs had a large amount of imprinted sites that could be accessed by template with less resistance. In addition, the thin layers of MIPs showed rapid mass transport. The adsorption rate slowed as the time went on because the imprinted cavity was constantly occupied, and eventually the adsorption equilibrium was reached. Furthermore, the non-linear forms of the pseudo-first-order kinetic model (3) and pseudo-second-order kinetic model (4) were applied to fit the as-obtained adsorption kinetic data.

$$Q_t = Q_e(1 - exp(-k_1 t)) \quad (3)$$

$$Q_t = Q_e^2 k_2 t/(1 + Q_e k_2 t) \quad (4)$$

where Q_e (mg g^{-1}) and Q_t (mg g^{-1}) are the adsorption amount of protein at equilibrium and time *t* (min), respectively. k_1 (min^{-1}) and k_2 (g min^{-1} mg^{-1}) represent the pseudo-first-order and pseudo-second-order kinetic rate constants, respectively. As depicted in Fig. 4B, Fig. S6 and Table S1, the pseudo-first-order kinetic model fit the as-obtained data of both two adsorbents quite well based on the higher correlation coefficient (r^2). Moreover, the Q_e of MIPs (84.1 mg g^{-1}) calculated by the pseudo-first-order kinetic model was also close to the as-obtained experimental data (81.1 mg g^{-1}). These results illustrated that the fast adsorption of template protein is due to the high density imprinted cavities on the surface of MIPs [35].

3.5. Binding isotherm

In order to estimate the binding capacities of the obtained polymers for BHb, the adsorption isotherm experiments were conducted. Good linearity was achieved for BHb (Fig. S7) and the limit of detection (LOD) of BHb for analysis by UV–vis spectroscopy was 2.5 μg mL^{-1}. As depicted in Fig. 4C, with the increase of initial concentration of BHb, the amount of BHb bound to MIPs increased rapidly, and then reached saturation over 0.20 mg mL^{-1}. Moreover, the binding capacity of MIPs was significantly higher than that of NIPs, suggesting that the imprinted sites of MIPs had better steric and chemical structure that matched with the template protein, while nonspecific effect was dominant for NIPs. Furthermore, the data of adsorption isotherm experiments were processed to evaluate the adsorption properties of obtained polymers according to the Langmuir (5) and Freundlich isotherm models (6).

$$C_e/Q_e = 1/(Q_{max}K_L) + C_e/Q_{max} \quad (5)$$

$$\log Q_e = n\log C_e + \log K_f \quad (6)$$

where C_e (mg mL^{-1}) is the equilibrium concentration of BHb. Q_e (mg g^{-1}) represents the protein amount bound to sorbents at equilibrium. Q_{max} (mg g^{-1}) is the maximum adsorption amount of sorbents in theory. K_L (mL mg^{-1}), K_f (mg g^{-1}) and *n* represent the Langmuir

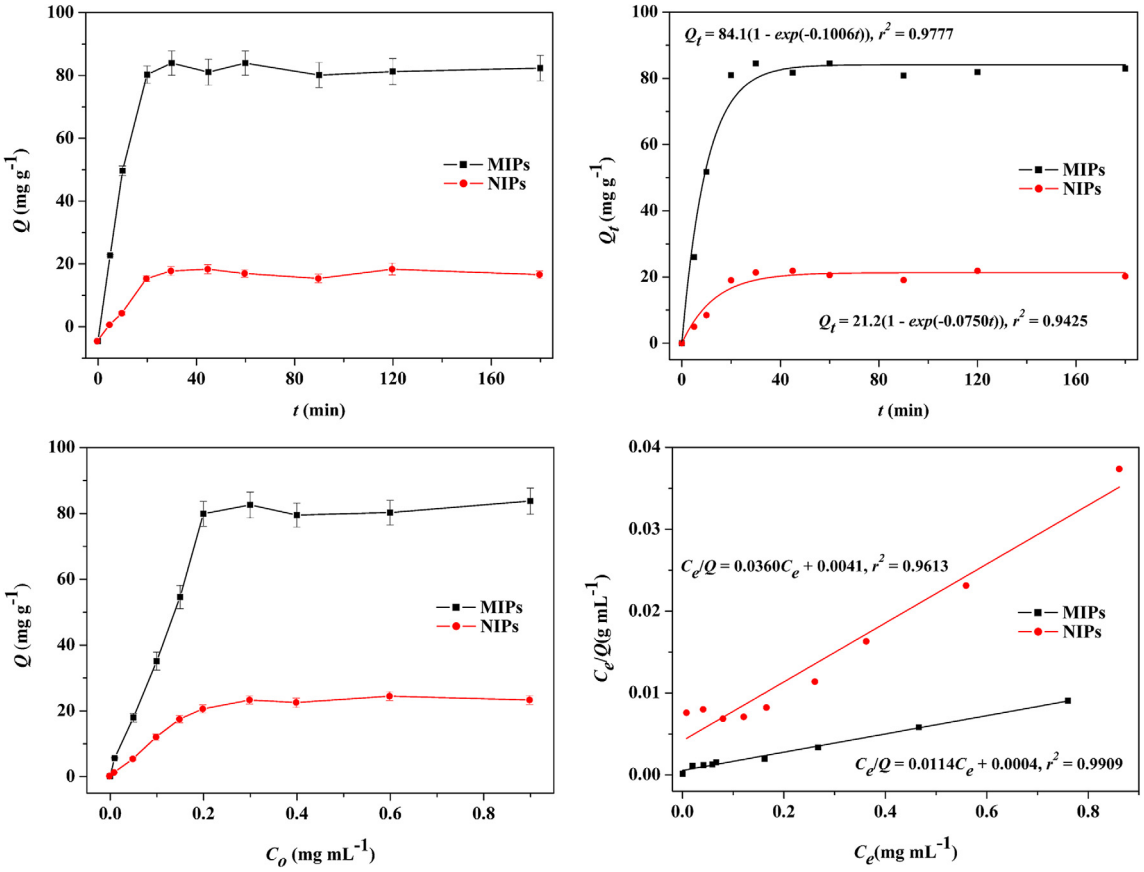

Fig. 4. (A) Adsorption kinetics, (B) The experimental kinetic data were fitted by the pseudo-first-order kinetic model, (C) Adsorption isotherms, (D), The adsorption isotherm experiments data were fitted by the Langmuir isotherm model.

constant, Freundlich constant and heterogeneity factor, respectively. The calculated fitting parameters were detailed in Fig. 4D, Fig. S8 and Table S2. Through comparison of the values of r^2, the Langmuir isotherm model was more suitable for fitting the adsorption behavior of MIPs and NIPs. Furthermore, the value of Q_{max} (87.7 mg g^{-1}) calculated by Langmuir isotherm model well agreed with that of obtained from experimental data (81.5 mg g^{-1}). These results illustrated that the bound BHb occurred on both MIPs and NIPs were monolayer and MIPs have higher adsorption amount than NIPs because of the imprinted sites [36].

3.6. Binding selectivity

The adsorption specific tests were conducted to estimate the selectivity of resultant materials and the results were detailed in Table S3. The results exhibit that the binding capacity of MIPs towards the template BHb (84.5 mg g^{-1}) was significantly higher than those of the other four non-template proteins (18.4–22.1 mg g^{-1}). Furthermore, the values of *IF* for BHb, BSA, Mb, OVA and Lyz were calculated as 3.95, 1.57, 1.28, 1.38 and 1.27, respectively, suggesting that the resultant MIPs had specific adsorption sites toward template protein. The reason could be that the size difference between the five proteins caused the adsorption capacity gaps, and the pI was also one of the factors that affect the selectivity of the MIPs [37]. There results demonstrated that the imprinted layers formed during the course of imprinting played an important role for selectively binding the template proteins. In addition, Table 1 listed the comparison of various BHb detection method based on magnetic MIPs, which have been widely used. The resultant photonic and magnetic dual responsive MIPs not only show good adsorption amount and selectivity, but also have unique optical properties, which can facilitate the release of protein under the irradiation of 365 nm light and reduce the elution time.

3.7. Photoregulated uptake and release of protein

As listed in Table S4, the four proteins have good stability under irradiation at 365 nm and 440 nm for 2 h with the RSD values less than 0.58%. Moreover, the photoisomerization reversibility of the resultant MIPs was estimated by the photoregulated uptake and release experiments and the binding behaviors to the four proteins were revealed in Fig. 5. In the dark, the resultant MIPs showed high adsorption capacity toward the template protein BHb (66.7%) due to the imprinted sites formed during the polymerization. After irradiated with 365 nm light for 2 h, 31.4% BHb was released from MIPs, which could be attributed to the change in the imprinted sites by the *trans-cis* isomerization of azobenzene chromophores under photoinduction [33]. On the contrary, under irradiation at 440 nm, BHb was rebound into the MIPs with the adsorption amount of 67.2% after 2 h, which was due to the imprinted sites turning to original through the photoinduced *cis-trans* isomerization of functional monomer MAPASA. These similar results were observed by repeated the photoswitching irradiation at 365 and 440 nm, suggesting that the substrate affinity of the imprinted sites were reversible in the course of photoinduced isomerization of MAPASA. Moreover, the changes in uptake and release of other three proteins were not significant under the same condition, indicating that the resultant MIPs had a satisfactory selective photoresponsive ability to the template protein.

3.8. Actual sample analysis

SDS-PAGE was used to confirm the practicability and selectivity of the resultant MIPs and the results were released in Fig. 6. Lanes 1 and 4

Table 1
The comparison of various BHb detection method based on magnetic MIPs.

Magnetic carrier	Q_{max} (mg g^{-1})	*IF*	Elution conditions	Elution time	Reference
γ-Fe_2O_3@CHO	93.1	3.85	5% SDS solution containing 2% oxalic acid	3 h	[38]
Fe_3O_4@NH_2	34.5	4.79	0.1 mol L^{-1} NaOH	3 h	[37]
Fe_3O_4@Au	89.1	3.42	10% acetic acid	–	[39]
Fe_3O_4@COOH	75.7	4.02	2% SDS-HAc (2%)	2 h	[40]
Fe_3O_4@SiO_2	77.6	2.30	10% acetic acid containing 10% SDS solution	–	[41]
Fe_3O_4@SiO_2	84.5	3.95	2% SDS-HAc solution under 365 nm irradiation	1 h	This work

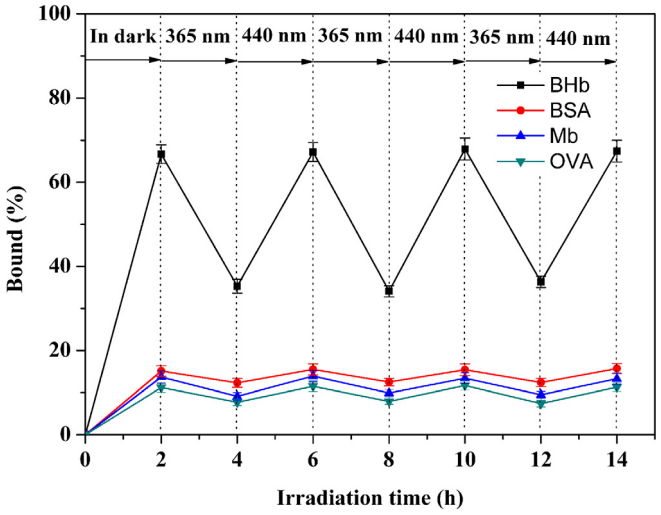

Fig. 5. Photoregulated release and uptake of BHb, BSA, Mb and OVA by the MIPs.

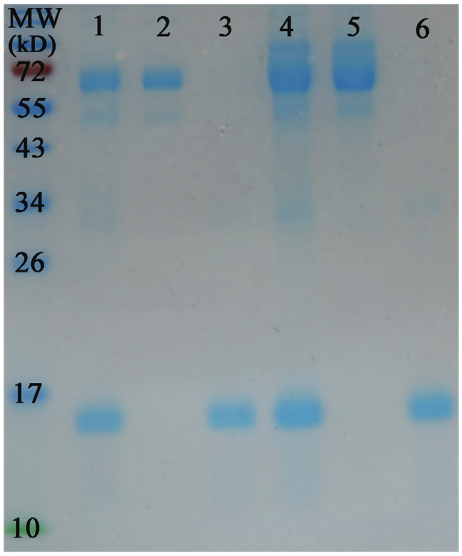

Fig. 6. SDS-PAGE analysis to evaluate the applicability of MIPs. Lane 1, 0.25 mg mL^{-1} of BHb and BSA binary solution; lane 2, remaining BHb and BSA solution after adsorption by MIPs; lane 3, the bound standard protein mixture eluted by 2% SDS-HAc solution; lane 4, bovine blood diluted 150-fold; lane 5, remaining bovine blood after adsorption by MIPs; lane 6, the adsorbed bovine blood eluted by 2% SDS-HAc solution.

were the mixed proteins of BHb and BSA (0.25 mg mL^{-1} for each) and bovine blood sample diluted 150-fold with Tris-HCl buffer (pH = 7.0, 10 mM), respectively. When the mixed proteins and diluted bovine blood sample were adsorbed by resultant MIPs in the dark, BHb was almost completely removed from lanes 2 and 5. After eluting the MIPs bound the mixture protein solution and diluted bovine blood sample

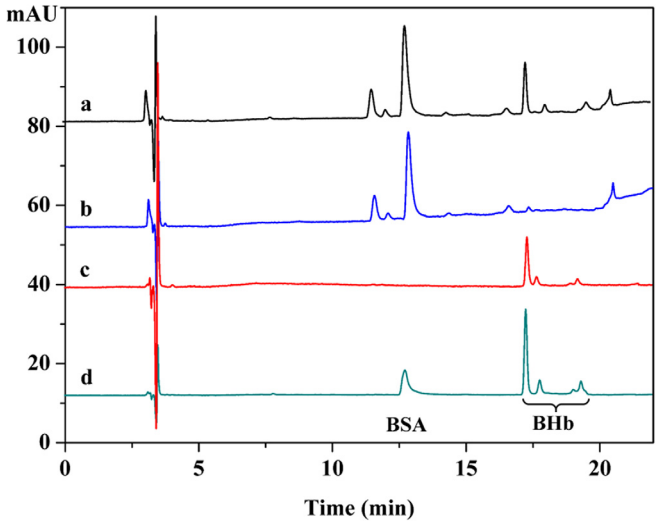

Fig. 7. Chromatograms of bovine blood solution diluted 150-fold (a), remaining bovine blood solution diluted 150-fold after adsorption by MIPs (b), eluted the adsorbed MIPs (c) and standard mixed solution of BSA and BHb (d).

with optimized 2% SDS-HAc solution (Fig. S9) under irradiation at 365 nm, the BHb band reappeared in lanes 3 and 6, respectively.

Moreover, the practical applicability was also evaluated by HPLC analysis. The chromatograms of bovine blood solution diluted 150-fold (curve a), adsorbed by MIPs (curve b), eluted the adsorbed MIPs (curve c) and standard mixed proteins of BSA and BHb (curve d) were shown in Fig. 7. The peak of BHb was not a single peak, which was accordance with other work [42]. The reason was that BHb consisted of four polypeptide chains, which were dissociated by the organic solvent in the mobile phase. It could be seen that BHb existed in the bovine blood sample with the complex matrix (curve a). After adsorbed by MIPs, BHb was almost completely removed (curve b) from the bovine blood sample. The selectively adsorbed BHb was reacquired from the elution solvent (curve c). These results of SDS-PAGE and HPLC analysis demonstrated the remarkable specific selectivity of the resultant MIPs toward the template BHb from complex biological samples.

4. Conclusions

In summary, novel photonic and magnetic dual responsive protein MIPs were successfully developed in biocompatible aqueous media by surface polymerization for the recognition of BHb. The resultant MIPs not only showed outstanding magnetic properties for rapid separation, but also exhibited well selective photoreponsive ability towards template protein by alternated irradiation with 365 and 440 nm light. Meanwhile, the resultant MIPs also revealed fast adsorption kinetics, high binding capacity and good selectivity. Furthermore, the MIPs were successfully applied to specifically extract template protein from actual biological sample. All these results of this work demonstrated the practicality to fabricate photonic and magnetic dual responsive protein MIPs in biocompatible aqueous media and this material would have a wide application prospect in specific recognition and determination of

proteins in complex biological samples.

Acknowledgements

We gratefully acknowledge the National Natural Science Foundation of China (No. 81503033), the Natural Science Foundation of Shaanxi Province (No. 2016JQ8016) and the Fundamental Research Funds for the Central Universities (No. xjj2018222) for financial support.

Appendix A. Supplementary data

Supplementary data to this article can be found online at https://doi.org/10.1016/j.cej.2019.04.019.

References

[1] L. Duan, Q. He, X. Yan, Y. Cui, K. Wang, J. Li, Hemoglobin protein hollow shells fabricated through covalent layer-by-layer technique, Biochem. Biophys. Res. Commun. 354 (2007) 357–362.
[2] X. Wang, S. Yu, W. Liu, L. Fu, Y. Wang, J. Li, L. Chen, Molecular imprinting based hybrid ratiometric fluorescence sensor for the visual determination of bovine hemoglobin, ACS Sens. 3 (2018) 378–385.
[3] M.D. Hoban, S.H. Orkin, D.E. Bauer, Genetic treatment of a molecular disorder: gene therapy approaches to sickle cell disease, Blood 127 (2016) 839–848.
[4] S.W. Chuang, J. Rick, T.C. Chou, Electrochemical characterisation of a conductive polymer molecularly imprinted with an Amadori compound, Biosen. Bioelectron. 24 (2009) 3170–3173.
[5] C. Iino, T. Mikami, T. Igarashi, T. Aihara, K. Ishii, J. Sakamoto, H. Tono, S. Fukuda, Evaluation of scoring models for identifying the need for therapeutic intervention of upper gastrointestinal bleeding: a new prediction score model for Japanese patients, Digest. Endosc. 28 (2016) 714–721.
[6] M.V. Gayalas, A. Breskin, M. Yuzefpolskaya, A. Eisenberger, F. Castagna, R.T. Demmer, M. Flannery, A.R. Garan, K. Takeda, H. Takayama, Y. Naka, V.K. Topkara, P.C. Colombo, Discriminatory performance of positive urine hemoglobin for detection of significant hemolysis in patients with continuous-flow left ventricular assist devices, J. Heart Lung Transpl. 36 (2017) 59–63.
[7] T.S. Anirudhan, S. Alexander, A potentiometric sensor for the trace level determination of hemoglobin in real samples using multiwalled carbon nanotube based molecular imprinted polymer, Eur. Polym. J. 97 (2017) 84–93.
[8] P.A. Beer, P.J. Campbell, L.M. Scott, A.J. Bench, W.N. Erber, D. Bareford, B.S. Wilkins, J.T. Reilly, H.C. Hasselbalch, R. Bowman, K. Wheatley, G. Buck, C.N. Harrison, A.R. Green, MPL mutations in myeloproliferative disorders: analysis of the PT-1 cohort, Blood 112 (2008) 141–149.
[9] Y.Q. Wang, H.M. Zhang, Q.H. Zhou, Studies on the interaction of caffeine with bovine hemoglobin, Eur. J. Med. Chem. 44 (2009) 2100–2105.
[10] Y. Zhang, M. Zhang, J. Yang, L. Ding, J. Zheng, J. Xu, Facile synthesis of sea urchin-like magnetic copper silicate hollow spheres for efficient removal of hemoglobin in human blood, J. Alloy. Compd. 695 (2017) 3256–3266.
[11] M. Zhang, Y. Wang, Y. Zhang, L. Ding, J. Zheng, J. Xu, Preparation of magnetic carbon nanotubes with hierarchical copper silicate nanostructure for efficient adsorption and removal of hemoglobin, Appl. Surf. Sci. 375 (2016) 154–161.
[12] L. Chen, S. Xu, J. Li, Recent advances in molecular imprinting technology: current status, challenges and highlighted applications, Chem. Soc. Rev. 40 (2011) 2922–2942.
[13] R. Schirhagl, Bioapplications for molecularly imprinted polymers, Anal. Chem. 86 (2014) 250–261.
[14] L. Chen, X. Wang, W. Lu, X. Wu, J. Li, Molecular imprinting: perspectives and applications, Chem. Soc. Rev. 45 (2016) 2137–2211.
[15] A. Martin-Esteban, Molecularly-imprinted polymers as a versatile, highly selective tool in sample preparation, Trend. Anal. Chem. 45 (2013) 169–181.
[16] A. Zamora-Galvez, A. Ait-Lahcen, L.A. Mercante, E. Morales-Narvaez, A. Amine, A. Merkoci, Molecularly imprinted polymer-decorated magnetite nanoparticles for selective sulfonamide detection, Anal. Chem. 88 (2016) 3578–3584.
[17] F. Chen, J. Wang, R. Lu, H. Chen, X. Xie, Fast and high-efficiency magnetic surface imprinting based on microwave-accelerated reversible addition fragmentation chain transfer polymerization for the selective extraction of estrogen residues in milk, J. Chromatogr. A 1562 (2018) 19–26.
[18] C. Boitard, A. Bee, C. Menager, N. Griffete, Magnetic protein imprinted polymers: a review, J. Mater. Chem. B 6 (2018) 1563–1580.
[19] M. Dabrowski, P. Lach, M. Cieplak, W. Kutner, Nanostructured molecularly imprinted polymers for protein chemosensing, Biosen. Bioelectron. 102 (2018) 17–26.
[20] X.Y. Zhang, N. Zhang, C.B. Du, P. Guan, X.M. Gao, C.Y. Wang, Y.F. Du, S.C. Ding, X.L. Hu, Preparation of magnetic epitope imprinted polymer microspheres using cyclodextrin-based ionic liquids as functional monomer for highly selective and effective enrichment of cytochrome c, Chem. Eng. J. 317 (2017) 988–998.
[21] W. Li, Y. Sun, C.C. Yang, X.M. Yan, H. Guo, G.Q. Fu, Fabrication of surface protein-imprinted nanoparticles using a metal chelating monomer via aqueous precipitation polymerization, ACS Appl. Mater. Inter. 7 (2015) 27188–27196.
[22] F.F. Yang, D.D. Deng, X.C. Dong, S. Lin, Preparation of an epitope-imprinted polymer with antibody-like selectivity for beta2-microglobulin and application in serum sample analysis with a facile method of on-line solid-phase extraction coupling with high performance liquid chromatography, J. Chromatogr. A 1494 (2017) 18–26.
[23] A.K. Mandal, M. Gangopadhyay, A. Das, Photo-responsive pseudorotaxanes and assemblies, Chem. Soc. Rev. 44 (2015) 663–676.
[24] R. Deloncle, A.M. Caminade, Stimuli-responsive dendritic structures: The case of light-driven azobenzene-containing dendrimers and dendrons, J. Photochem. Photobiol. C 11 (2010) 25–45.
[25] S. Xu, H. Lu, X. Zheng, L. Chen, Stimuli-responsive molecularly imprinted polymers: versatile functional materials, J. Mater. Chem. C 1 (2013) 4406–4422.
[26] F. Chen, Y. Dong, Y. Zhao, Synthesis and characterization of photo-responsive magnetic molecularly imprinted microspheres for the detection of sulfonamides in aqueous solution, J. Sep. Sci. 39 (2016) 4866–4875.
[27] Q. Hu, Y. Bu, X. Zhen, K. Xu, R. Ke, X. Xie, S. Wang, Magnetic carbon nanotubes camouflaged with cell membrane as a drug discovery platform for selective extraction of bioactive compounds from natural products, Chem. Eng. J. 364 (2019) 269–279.
[28] Y. Zhang, M. Zhang, J. Yang, L. Ding, J. Zheng, J. Xu, S. Xiong, Formation of Fe_3O_4@SiO_2@C/Ni hybrids with enhanced catalytic activity and histidine-rich protein separation, Nanoscale 8 (2016) 15978–15988.
[29] H.J. Zhu, H. Yao, K.X. Xia, J.X. Liu, X.L. Yin, W.L. Zhang, J.M. Pan, Magnetic nanoparticles combining teamed boronate affinity and surface imprinting for efficient selective recognition of glycoproteins under physiological pH, Chem. Eng. J. 346 (2018) 317–328.
[30] J.P. Fan, J.X. Yu, X.M. Yang, X.H. Zhang, T.T. Yuan, H.L. Peng, Preparation, characterization, and application of multiple stimuli-responsive rattle-type magnetic hollow molecular imprinted poly (ionic liquids) nanospheres (Fe_3O_4@void@PILMIP) for specific recognition of protein, Chem. Eng. J. 337 (2018) 722–732.
[31] Y. Bu, Q. Hu, R. Ke, S. Yue, X. Xie, S. Wang, Cell membrane camouflaged magnetic nanoparticles as a biomimetic drug discovery platform, Chem. Commun. 54 (2018) 13427–13430.
[32] X. Xie, X. Pan, S. Han, S. Wang, Development and characterization of magnetic molecularly imprinted polymers for the selective enrichment of endocrine disrupting chemicals in water and milk samples, Anal. Bioanal. Chem. 407 (2015) 1735–1744.
[33] C. Gong, K.L. Wong, M.H.W. Lam, Photoresponsive molecularly imprinted hydrogels for the photoregulated release and uptake of pharmaceuticals in the aqueous media, Chem. Mater. 20 (2008) 1353–1358.
[34] Y. Wei, Q. Zeng, S. Bai, M. Wang, L. Wang, Nanosized difunctional photo responsive magnetic imprinting polymer for electrochemically monitored light-driven paracetamol extraction, ACS Appl. Mater. Inter. 9 (2017) 44114–44123.
[35] H.H. Xiong, X.Q. Wu, W.H. Lu, J.Q. Fu, H.L. Peng, J.H. Li, X.Y. Wang, H. Xiong, L.X. Chen, Switchable zipper-like thermoresponsive molecularly imprinted polymers for selective recognition and extraction of estradiol, Talanta 176 (2018) 187–194.
[36] H.R. Ali, H.H. El-Maghrabi, F. Zahran, Y.M. Moustafa, A novel surface imprinted polymer/magnetic hydroxyapatite nanocomposite for selective dibenzothiophene scavenging, Appl. Surf. Sci. 426 (2017) 56–66.
[37] R. Gao, X. Mu, J. Zhang, Y. Tang, Specific recognition of bovine serum albumin using superparamagnetic molecularly imprinted nanomaterials prepared by two-stage core-shell sol-gel polymerization, J. Mater. Chem. B 2 (2014) 783–792.
[38] Y. Hao, R. Gao, D. Liu, B. Zhang, Y. Tang, Z. Guo, Preparation of biocompatible molecularly imprinted shell on superparamagnetic iron oxide nanoparticles for selective depletion of bovine hemoglobin in biological sample, J. Colloid Interf. Sci. 470 (2016) 100–107.
[39] Y. Li, Y. Chen, L. Huang, B. Lou, G. Chen, Creating BHb-imprinted magnetic nanoparticles with multiple binding sites, Analyst 142 (2017) 302–309.
[40] R. Gao, Y. Hao, L. Zhang, X. Cui, D. Liu, M. Zhang, Y. Tang, Y. Zheng, A facile method for protein imprinting on directly carboxyl-functionalized magnetic nanoparticles using non-covalent template immobilization strategy, Chem. Eng. J. 284 (2016) 139–148.
[41] M. Zhang, Y. Wang, X. Jia, M. He, M. Xu, S. Yang, C. Zhang, The preparation of magnetic molecularly imprinted nanoparticles for the recognition of bovine hemoglobin, Talanta 120 (2014) 376–385.
[42] J. Liu, Y. Liang, J. Shen, Q. Bai, Polymeric ionic liquid-assembled graphene-immobilized silica composite for selective isolation of human serum albumin from human whole blood, Anal. Bioanal. Chem. 410 (2018) 573–584.